Eur. Phys. J. D **4**, 47–56 (1998)

THE EUROPEAN PHYSICAL JOURNAL D

Stimulated Raman adiabatic passage with amplitude modulated fields

L.P. Yatsenko[1,a], B.W. Shore[1,b], K. Bergmann[1,c], and V.I. Romanenko[2]

[1] Fachbereich Physik der Universität, 67653 Kaiserslautern, Germany
[2] Institute of Physics, National Academy of Sciences of Ukraine, prospekt Nauky, 46, 252650, Kiev-22, Ukraine

Received: 25 February 1998 / Revised: 5 May 1998 / Accepted: 2 July 1998

Abstract. We discuss stimulated Raman adiabatic passage (STIRAP) for pulses whose amplitude is modulated with constant frequency. We discuss in detail the case of a Lambda (Raman) system driven by two amplitude-modulated pulses. We present a variety of numerical solutions to the relevant Schrödinger equation, which we interpret using the Floquet theorem for the solution of systems of linear equations with periodic coefficients, the concept of quasienergies, and the assumption of adiabatic evolution. We find thresholds for successful population transfer and show that some peculiarities of the depicted efficiency of population transfer can be interpreted as pairs of Landau-Zener transitions in the areas of avoided crossings of quasienergies. We provide an analytic expression for the transfer efficiency in these cases. We show that the efficiency of population transfer is much more sensitive to the population decay from the upper level than in the case of smooth (non modulated) laser pulses. We note the applicability of the results to cases beyond the rotating wave approximation.

PACS. 32.80.Wr Other multiphoton processes – 42.50.Ct Quantum description of interaction of light and matter; related experiments

1 Introduction

Amongst the various techniques which permit the complete transfer of population between two quantum states, that of stimulated Raman adiabatic passage (STIRAP) has particular advantages for robustness [1–3]. In essence, this procedure uses a pump pulse (near resonant with transition 1-2) and a Stokes pulse (near resonant with transition 2-3) to achieve complete transfer of population between states 1 and 3. For this to occur, it is important that the Stokes pulse interact first (counterintuitive pulse order), that the pulses satisfy a few simple constraints on peak value and smoothness, and that the pulse frequencies together satisfy a two-photon resonance condition.

Although the STIRAP process is surprisingly robust (*e.g.* it does not require specific pulse shapes or pulse areas), there are known experimental effects which diminish population transfer. Very early in the experimental studies of the STIRAP process it was found that fluctuations in pulse amplitude could be detrimental [4]. Indeed, it is essential that the bandwidths of pulses to be used for STIRAP be very close to the Fourier transform limit. It might be supposed that any rapid variation of pulse envelope would, by increasing the pulse bandwidth, diminish transfer of population, because conditions for adiabatic evolution may fail. We here examine some special cases in which this simple view is incorrect. In doing so, we provide illustrations of the usefulness of adiabatic Floquet analysis in describing the STIRAP process.

Incoherent fluctuations are generally detrimental to any process, STIRAP included, which relies on maintaining coherence. We shall discuss cases of coherent variation, and we shall show that these are not always detrimental. The particular examples we use are of a pulse which has a sinusoidal modulation imposed on the otherwise slowly varying envelope. When the modulation is slow, then one expects (and finds) that the excitation differs little from what would occur without modulation. As the modulation increases in frequency the field changes become more rapid, and the usual conditions for adiabatic evolution (*i.e.* slowly changing interaction) fail. Nevertheless, we show that the STIRAP population transfer can sometimes succeed even then.

We begin by reviewing the STIRAP process, with a discussion of adiabatic evolution. This latter provides the usual understanding of how coherent excitation by slowly varying pulses affects atomic excitation. We then define modulated pulses and present examples of numerical

[a] *Permanent address*: Institute of Physics, National Academy of Sciences of Ukraine, prospekt Nauky, 46, 252650, Kiev-22, Ukraine.
[b] *Permanent address*: Lawrence Livermore National Laboratory, Livermore, CA 94550, USA.
[c] e-mail: `bergmann@rhrk.uni-kl.de`

integration of the Schrödinger equation. The results exhibit some features which, at first glance, seem unexpected. To explain features of these results we introduce adiabatic Floquet states, a generalization of the more traditional Floquet analysis valid for perfectly periodic Hamiltonians. This approach provides a simple explanation of the features.

The general approach used here has application to excitation in which the usual rotating wave approximation must be extended to include effects of counter-rotating terms. The final section presents an example.

2 Basic principles of STIRAP

2.1 RWA Hamiltonian

To establish basic definitions, we here review the STIRAP procedure. We consider three states, labeled 1, 2, 3, with energies $E_1 \leq E_3 < E_2$ (the so-called Lambda configuration) driven by two interactions, labeled P, S. Acting on this system is a local electric field which combines a pump pulse (carrier frequency ω_P) and a Stokes pulse (carrier frequency ω_S). As is customary, we make the rotating wave approximation (RWA). Upon defining a pair of single-step laser detunings of the carrier frequencies from their assigned Bohr transition frequencies,

$$\hbar\Delta_P \equiv (E_2 - E_1) - \hbar\omega_P, \qquad \hbar\Delta_S \equiv (E_2 - E_3) - \hbar\omega_S \tag{1}$$

a two-photon (Raman) detuning δ and an average detuning $\bar{\Delta}$,

$$\delta \equiv \Delta_P - \Delta_S, \qquad 2\bar{\Delta} \equiv \Delta_P + \Delta_S \tag{2}$$

we can write the basic RWA Hamiltonian matrix as

$$H(t) = \frac{\hbar}{2}\begin{bmatrix} -\delta & \Omega_P(t) & 0 \\ \Omega_P(t) & 2\bar{\Delta} & \Omega_S(t) \\ 0 & \Omega_S(t) & \delta \end{bmatrix}. \tag{3}$$

Note that our energy zero-point and our choice of the arbitrary phases of basis states [5] shifts all diagonal elements away from the common choice which sets $H_{11} = 0$.

The (time varying) Rabi frequencies $\Omega_P(t)$ and $\Omega_S(t)$ are, in the approach of the RWA, just products of dipole moments and electric field amplitudes, which can be taken as real slowly-varying functions of time.

2.2 Adiabatic states

The essence of adiabatic evolution and the elementary STIRAP process is that complete population transfer, between state ψ_1 and state ψ_3, can occur if certain simple conditions hold: (1) the two-photon resonance condition $\delta = 0$ holds for the Raman transition; (2) the Stokes pulse precedes the pump pulse and ceases first; and (3) the time evolution is adiabatic.

The theoretical analysis of the STIRAP process is most simply presented by first constructing the (three) instantaneous eigenstates $\Phi_n(t)$ of the RWA Hamiltonian $H(t)$ (the dressed states or adiabatic states)

$$[H(t) - \hbar\varpi_n(t)]\,\Phi_n(t) = 0. \tag{4}$$

When the two-photon detuning vanishes ($\delta = 0$) the eigenvalues are

$$\varpi_0(t) = 0, \qquad \varpi_\pm(t) = \tfrac{1}{2}\left[\bar{\Delta} \pm \sqrt{\bar{\Delta}^2 + \Omega(t)^2}\right], \tag{5}$$

where $\Omega(t)$ is the rms Rabi frequency,

$$\Omega(t) \equiv \sqrt{|\Omega_S(t)|^2 + |\Omega_P(t)|^2}. \tag{6}$$

(We retain these same labels $+, 0, -$ in the more general case when δ is not zero.) Then we express the statevector at each instant in terms of these dressed states,

$$\Psi(t) = \sum_{n=0,\pm} C_n(t) \exp\left[-i\int^t dt'\,\varpi_n(t')\right]\Phi_n(t). \tag{7}$$

At any time t the statevector $\Psi(t)$ is expressible as some combination of the adiabatic states $\Phi_n(t)$ appropriate to that time. In special cases (these are of particular interest) the statevector may be very nearly a single dressed state.

The usual approach to STIRAP is to find (three) dressed states at each instant. Initially, the system is in one of these states. Through suitable pulse construction, one allows the system to evolve adiabatically, meaning that the Rabi frequencies change only slowly and the system remains in this adiabatic state. The constraint on slow variation of the Rabi frequencies is that during the pulse action the differences of the eigenvalues always be much larger than the inverse of the pulse duration τ

$$|\varpi_k(t) - \varpi_m(t)| \gg \tau^{-1}, \quad k \neq m. \tag{8}$$

That is, to ensure adiabatic evolution it is necessary that the (three) eigenvalues remain well separated. When the detuning $\bar{\Delta}$ is small, the largest separation of the eigenvalues, ϖ_{max}, is half of the maximum value of the rms Rabi frequency,

$$\varpi_{max} \equiv \max|\varpi_k(t) - \varpi_m(t)| = \frac{1}{2}\max\Omega(t). \tag{9}$$

When the two-photon detuning vanishes ($\delta = 0$) the null-eigenvalue dressed state has the simple construction

$$\Phi_0(t) = \frac{1}{\Omega(t)}\begin{bmatrix} \Omega_S(t) \\ 0 \\ -\Omega_P(t) \end{bmatrix}. \tag{10}$$

Because this state has never any component of the excited state ψ_2, from which spontaneous emission occurs as a probability loss, it is known as a "trapped state" or "dark

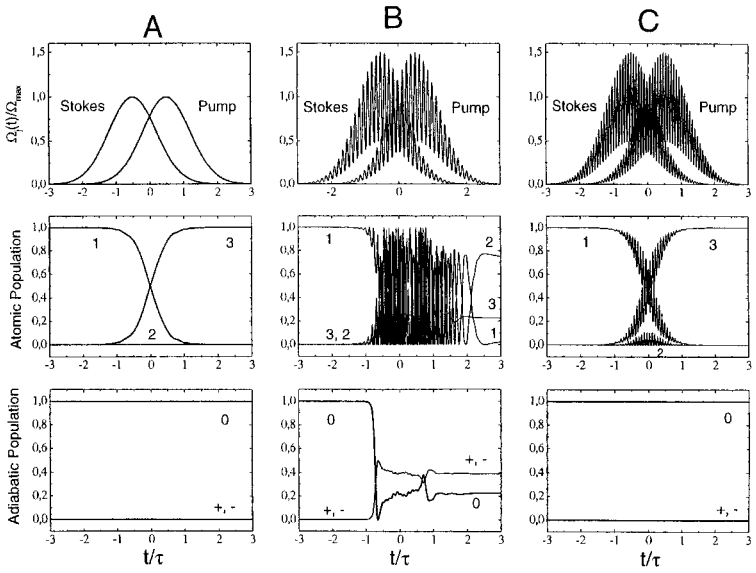

Fig. 1. Examples of excitation produced by pump-Stokes Gaussian pulses $f_G(t)$. Top frames show pulse envelopes *vs.* time, central frames show (atomic state) populations *vs.* time, bottom frames show probabilities of adiabatic states *vs.* time. All pulses are Gaussian, with $\tau_D = \tau$, pulse areas $\Omega_{max}\tau = 100$ and modulation phases $\phi_P = 0$, $\phi_S = 0.3\pi$. There is no loss. (A) Excitation by unmodulated pulses, $a_P = a_S = 0$. (B) Modulation at frequency $\omega_M = 0.5\Omega_{max}$, with $a_S = a_P = 0.5$. (C) Modulation at frequency $\omega_M = 0.8\Omega_{max}$, with $a_S = a_P = 0.5$.

state". With the use of a counterintuitive pulse sequence (Stokes before pump) this adiabatic state has the property

$$\psi_1 = \underset{init}{\longleftarrow}\Phi_0(t)\underset{final}{\longrightarrow} = -\psi_3 \tag{11}$$

Thus by starting in state ψ_1 and maintaining adiabatic conditions, population transfer is complete.

3 Numerical results

The object of principle interest is the population transfer efficiency of the pulse sequence. By definition, this is the population in the target state ψ_3 at the end of the pulses, assuming that all population originally resided in state ψ_1. A desirable scenario is when this efficiency is very close to unity. We regard the transfer to be poor when it is small.

It is not difficult to compute numerical solutions to the time-dependent Schrödinger equation for a variety of pulse shapes and modulations (we use the fourth order Runge-Kutta integration method), and to view the population histories which result from such computations. Such plots often provide useful insight into reasons for success or failure of population transfer.

3.1 Modulated pulses

We consider pulses $\Omega_j(t)$ which, in addition to having a slowly varying envelope $\Omega_j^{(0)}(t)$, are sinusoidally modulated with frequency ω_M,

$$\Omega_j(t) = \Omega_j^{(0)}(t)[1 + a_j\cos(\omega_M t + \varphi_j)], \quad (j = P, S). \tag{12}$$

For simplicity we assume that both pulses have the same peak value Ω_{max},

$$\Omega_S^{(0)}(t) = \Omega_{max} f_S(t), \qquad \Omega_P^{(0)}(t) = \Omega_{max} f_P(t), \tag{13}$$

by introducing envelope functions $f_j(t)$ having unit peak value, $\max|f_j(t)| = 1$. For simplicity we take the pump and Stokes pulses to have the same envelope functions, with the pump delayed from the Stokes pulse by time τ_D.

For the numerical examples we use Gaussian pulses,

$$f_P(t) = f_G(t - \tau_D/2), \quad f_S(t) = f_G(t + \tau_D/2),$$
$$f_G(t) \equiv \exp[-(t/\tau)^2], \tag{14}$$

although we will also make use of other pulse shapes in our discussion. To illustrate an extreme case of adiabatic eigenvalues we consider the pulses

$$f_P(t) = \sin(\pi t/2\tau), \quad f_S(t) = \cos(\pi t/2\tau) \tag{15}$$

to be used in the interval $0 < t < \tau$. To allow simple analytic expressions we consider linear-ramp pulses

$$f_P(t) = \left(\frac{1}{2} + \frac{t}{\tau}\right), \quad f_S(t) = \left(\frac{1}{2} - \frac{t}{\tau}\right) \tag{16}$$

in the interval $-\tau/2 < t < +\tau/2$: the Stokes pulse starts at a finite value and decreases linearly to zero, while the pump pulse rises linearly from zero.

3.2 Population histories

Figure 1 shows three examples of numerical solutions of the Schrödinger equation for three situations, chosen to illustrate particular points. The conditions for the cases differ in the chosen modulation frequency.

The first column, Figure 1A, shows a typical example of the usual three-state STIRAP (*i.e.* unmodulated pulses). The top frame shows the two overlapping pulse envelopes (Gaussians), with the Stokes preceding the pump. The middle frame shows the (three) time varying populations. We see that the population in (initial) state ψ_1 drops monotonically to zero during the overlap time,

while the population in (target) state ψ_3 rises monotonically to unity during this interval. Very little population enters the intermediate state ψ_2.

The lower frame on this figure plots the probability of finding the system in the several dressed adiabatic states. (These states, discussed below, are adiabatic Floquet states, the generalization of the adiabatic states used for ordinary STIRAP.) We see that these remain constant: the system begins in the trapped state (0) and remains in this state.

The middle column, Figure 1B, shows an example of behavior when the pulses of Figure 1A are modulated at a frequency approaching the peak Rabi frequency (the modulation frequency here is $\omega_M = 0.5\Omega_{max}$). The top frame shows the modulated pulses, which exhibit rapid variation in amplitude. The central frame shows the population in the three atomic states. As can be seen, for the conditions chosen here there is poor population transfer to state ψ_3, and the population undergoes rapid irregular changes during the pulse overlap. The rapid variations originate with both the Rabi frequencies and the modulation frequency.

The lower frame plots the probability of remaining in an adiabatic state. Unlike the previous case, here there are visible distinct changes. At particular times there occur abrupt changes in the Floquet state populations, and at the end there occurs little population in the desired state Φ_0.

It might be thought that the failure to produce efficient population transfer, as occurs in this second set of figures, is an inevitable outcome of introducing rapid variation of the pulse amplitude. That this view is too simplistic can be seen from the three final frames, Figure 1C. Here the modulation has been increased somewhat (to $\omega_M = 0.8\Omega_{max}$) and the pulse envelopes appear even more strongly variable – steeper slopes and more rapid variation. However, we see in the central frame that population transfer is successful. Although there is noticeable high-frequency modulation upon the population histories, it is clear that the STIRAP process succeeds in this case.

The lower frame plots the probability of remaining in an adiabatic Floquet state. As with the first frames, the constancy of these probabilities signifies good population transfer.

It is not difficult to compute population histories for a variety of pulse modulations, and to organize these computations into plots of transfer efficiency (the population in state ψ_3 at the end of the pulse sequence) for a variety of pulse parameters. Viewing such plots one can infer the conditions (of modulation and amplitude) needed to produce population transfer. Given pulses which are sufficiently intense that STIRAP would succeed with smooth pulses (specifically, the pulse area $\Omega_{max}\tau$ must be much larger than 1), what matters is how large the modulation frequency ω_M is compared with Ω_{max}.

3.3 Variation of ω_M and Ω_{max}

Figure 2 presents an example of population transfer efficiency, for fixed peak Rabi frequencies and pulse delay, as a function of modulation frequency ω_M, for a lossless system and Gaussian pulses.

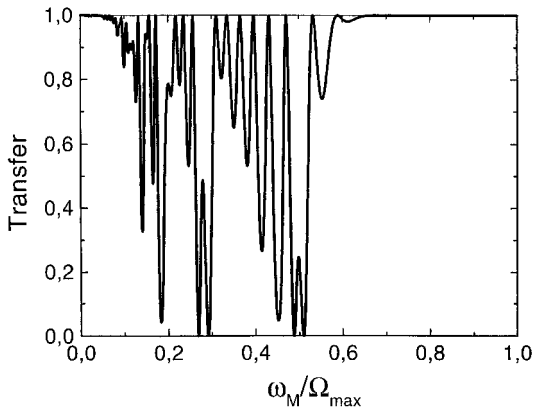

Fig. 2. Population transfer (to state 3) *vs.* ω_M/Ω_{max}. See that small modulation frequency ω_M is good, large ω_M is good, and for intermediate values there are some regularities. Parameters: Gaussian pulses, $\tau_D = \tau$, pulse area $\Omega_{max}\tau = 100$, modulation amplitude $a_P = a_S = 0.5$, phases $\phi_P = 0$, $\phi_S = 0.3\pi$, no loss.

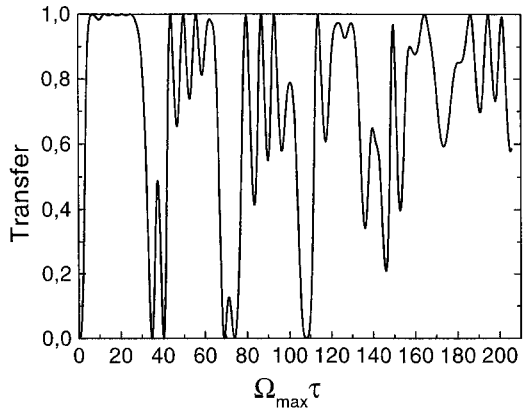

Fig. 3. Population transfer *vs.* $\Omega_{max}\tau$. See that small $\Omega_{max}\tau$ is bad (not adiabatic), large $\Omega_{max}\tau$ is good, and for large values there are regularities. Parameters: Gaussian pulses, $\tau_D = \tau$, modulation frequency $\omega_M\tau = 20$, modulation amplitude $a_P = a_S = 0.5$, phases $\phi_P = 0$, $\phi_S = 0.3\pi$, no loss.

It is quite evident that when the modulation frequency ω_M exceeds a critical value, momentarily denoted as ω_{crit}, good population transfer occurs. The critical value is seen to be slightly less than $0.7\Omega_{max}$. This general behavior, of a threshold modulation frequency, happens for any value of modulation amplitude a_S or a_P.

For slower modulation, $\omega_M < \omega_{crit}$, there will be found both good and poor population transfer, between zero and unity. The dependence of transfer efficiency upon modulation frequency shows definite patterns. We will comment below on the source of these regularities.

In the limit of very slow modulation, $\omega_M \ll \omega_{crit}$, one recovers the high transfer probability associated with conventional unmodulated STIRAP.

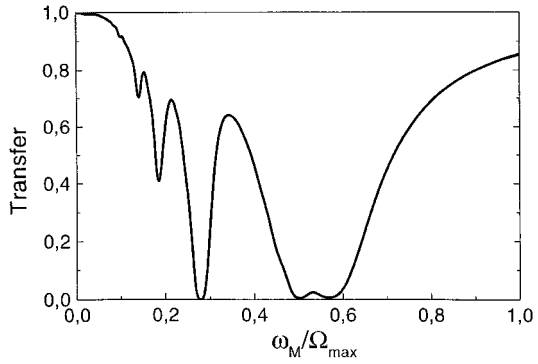

Fig. 4. Population transfer *vs.* ω_M/Ω_{max} in the presence of loss. See that features are less sharp and threshold is less pronounced. Parameters are similar to Figure 2 but with loss: Gaussian pulses, $\tau_D = \tau$, pulse area $\Omega_{max}\tau = 100$, modulation amplitude $a_P = a_S = 0.5$, phases $\phi_P = 0$, $\phi_S = 0.5\pi$, loss $\gamma\tau = 10$.

These results can be viewed in a complementary manner, holding the modulation frequency ω_M fixed while changing the peak Rabi frequency Ω_{max} (this amounts to varying the pulse fluency). Figure 3 shows the efficiency for varying $\Omega_{max}\tau$. We see that for very small Rabi frequency, poor transfer occurs. This is because the adiabatic criterion $\Omega_{max}\tau > 1$ is not satisfied; the pulse areas are too small to produce good adiabatic evolution. For somewhat larger Rabi frequencies, but bounded by the limit $0.7\Omega_{max} < \omega_M$, good transfer occurs. (Note: the factor 0.7 occurs because Ω_{max} is the peak Rabi frequency for one pulse. The plots depict the case $\omega_M\tau = 20$, so that the equality $0.7\Omega_{max} = \omega_M$ occurs for $0.7\Omega_{max}\tau = 20$.) When the Rabi frequency exceeds this value there occur highs and lows of transfer efficiency. For very large Rabi frequency, $\Omega_{max} \gg \omega_M$, the transfer efficiency is oscillatory but generally poor.

3.4 Effect of population loss

When there is population loss from state ψ_2 (as occurs by spontaneous emission to states other than ψ_1 or ψ_3) the transfer state (see Sect. 4.4) is lossy. Nevertheless, for some frequency conditions we have population trapping and no loss of probability. One can take the loss into account by the substitution $2\bar{\Delta} \to 2\bar{\Delta} - i\gamma$ in equation (4). When loss is present, the pattern of population transfer dependence on modulation frequency becomes more regular in the region of low efficiency. The boundary between high and low efficiency regimes becomes less clear cut. Oscillations occur as ω_M varies. Figure 4 illustrates this.

4 Analytic results and explanations

The various regularities of population transfer with amplitude modulated pulses can be understood by means of a simple generalization of conventional STIRAP. Whereas the usual case deals with a nearly static Hamiltonian, and uses plots of adiabatic energies to reveal crossings of diabatic curves which affect adiabatic evolution, here we deal with a nearly periodic Hamiltonian. We can use plots of appropriate eigenvalues, the adiabatic Floquet eigenvalues (or quasienergies) to reveal similar problems with adiabatic evolution with modulated pulses.

4.1 Floquet states

Prior to examining the problem of interest (modulated pulses) we first review the limiting case in which the Hamiltonian is, at all times, perfectly periodic, with period $T = 2\pi/\omega_M$. In this idealization the Schrödinger equation becomes a set of coupled linear ordinary differential equations with periodic coefficients (the matrix elements of the RWA Hamiltonian $H(t)$)

$$\hbar\frac{d}{dt}\Psi(t) = -iH(t)\Psi(t). \tag{17}$$

One can apply the Floquet theorem [6–11] to express any solution to such equations in the form

$$\Psi(t) = \sum_{n=1,\pm} \exp(-i\varpi_{0n}t)\tilde{\Phi}_n(t)C_n \tag{18}$$

where $\tilde{\Phi}_n(t)$, a Floquet state, is a periodic function, of period T , and $\hbar\varpi_{0n}$ (the quasienergy [7]) is an eigenvalue of the Floquet Hamiltonian $\mathcal{H}(t)$

$$\mathcal{H}(t)\tilde{\Phi}_n(t \equiv \left[H(t) - \hbar\frac{d}{dt}\right]\tilde{\Phi}_n(t) = \hbar\varpi_{0n}\tilde{\Phi}_n(t). \tag{19}$$

The constants C_n are chosen to force the function $\Psi(t)$ to satisfy given initial conditions.

Because the Floquet state $\tilde{\Phi}_n(t)$ is periodic it can be expanded in a Fourier series, leading to the construction

$$\Psi(t) = \sum_{n=0,\pm} C_n \sum_{m=-\infty,+\infty} \exp(-i\varpi_{0n}t - im\omega_M t)\varphi_{mn}. \tag{20}$$

The various Fourier components φ_{mn} are connected by the need to express an adiabatic Floquet state $\tilde{\Phi}_n(t)$.

Because there are three basis states, there are three quasienergies and three independent Floquet states $\tilde{\Phi}_n(t)$. However, the eigenvalues of the Floquet Hamiltonian form an infinite set: if $\hbar\varpi_{0n}$ is an eigenvalue, then so is $\hbar\varpi_{0n} + \hbar m\omega_M$, where m is any integer. The totality of eigenvalues form a succession of triads, separated by $\hbar\omega_M = 2\pi\hbar/T$. Floquet eigenvalues, say $\varpi_{mn} = \varpi_{0n} + m\omega_M$, bear two labels: an integer m, running from $-\infty$ to $+\infty$, which expresses the periodicity of the eigenvalues; and a three-valued label n which identifies, for given manifold (or zone) label m, which of three Floquet exponents (or quasienergies) is meant. It is common to use the labels $+, 0, -$ for this purpose.

4.2 Adiabatic Floquet theory

We can apply Floquet analysis to a slowly changing periodic Hamiltonian in exactly the same way we apply adiabatic theory to a nearly constant Hamiltonian. Let us consider a succession of contiguous intervals, each of duration T_0. The time T_0 must be small enough ($T_0 \ll \tau$) that during it the pulse amplitude can be regarded as a constant times a trigonometric function varying at frequency ω_M, yet long enough that the frequency ω_M is well defined, meaning that there occur many modulation periods within the interval T_0, or $T_0 \gg T$.

Under these conditions one can introduce a Floquet expansion within each time interval $t_{k-1} < t < t_k$ ($t_k = kT_0$, $k = 1, 2 \ldots$)

$$\Psi(t) \equiv \sum_{n=0,\pm} C_n^{(k-1)} \tilde{\Phi}_n^{(k-1)}(t) \times \exp\left[-i\varpi_{0n}^{(k-1)}(t - t_{k-1}) - iT_0 \sum_{m=0}^{k-1} \varpi_{0n}^{(m)}\right]. \quad (21)$$

The Floquet exponents $\varpi_{0n}^{(k)}$ vary from one interval to the next, as do the adiabatic Floquet states $\tilde{\Phi}_n^{(k)}(t)$. The coefficients $C_n^{(k)}$ differ from one interval to the next, and in that sense they become time dependent. They must be chosen so that $\Psi(t)$ obeys desired initial conditions and is continuous across boundaries of time segments. As with the quasistatic RWA Hamiltonian, we start with the statevector in one of the Floquet states. We require adiabatic evolution thereafter, so that the system remains in this state [11].

4.3 Adiabatic Floquet eigenvalues

Plots of (conventional) adiabatic eigenvalues can reveal regions where curves cross (or avoid crossing). These are regions where adiabatic evolution may fail. The same deductions can be made when viewing plots of adiabatic Floquet eigenvalues.

Figure 5 presents three examples of such eigenvalues, for Gaussian pulses with appropriately chosen delays. From left to right, the three frames present results for increasing Rabi frequency at fixed modulation frequency or, alternatively, for decreasing modulation frequency at fixed Rabi frequency.

Figure 5A shows an example of pulses whose peak Rabi frequency Ω_{max} is chosen such that ϖ_{max} is less than the modulation frequency ω_M. The curves separate into an infinite sequence of triads, each separated by ω_M. The plot shows three of these.

For successful adiabatic evolution one must remain in the null eigenvalue state.

When ϖ_{max} exceeds the modulation frequency, the sets of triads overlap. Figure 5B shows an example of such a case. As can be seen, the null eigenvalue state has, in this case, two times during the pulses when it nearly coincides with two other eigenvalues: there occur two avoided crossings, each involving three states. It is to be expected that adiabatic evolution may fail for such situations.

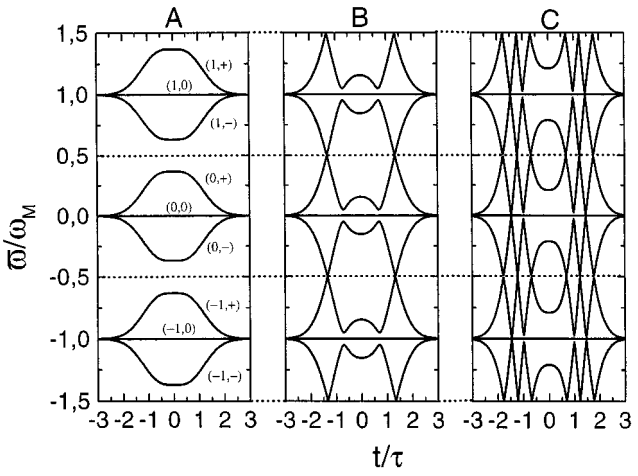

Fig. 5. Adiabatic Floquet eigenvalues (quasienergies) ϖ_{mn} *vs.* time for $m = -1, 0, +1$ and $n = +, 0, -$: (A) for weak excitation, $\omega_M = 1.5\Omega_{max}$; (B) for moderate excitation, $\omega_M = 0.5\Omega_{max}$; (C) for strong excitation, $\omega_M = 0.2\Omega_{max}$. Parameters: Gaussian pulses $\tau_D = \tau$, pulse area $\Omega_{max}\tau = 100$, modulation amplitude $a_P = a_S = 0.5$, phases $\phi_P = 0$, $\phi_S = 0.3\pi$, no loss $\gamma = 0$.

In this picture the curves from separate manifolds do not cross. At the times of avoided crossings the curves are separated by the modulation amplitude a. (This separation at the avoided crossing is analogous to the separation of the usual adiabatic curves near an avoided crossing; the parameter a acts here as does the diabatic interaction there.) As this amplitude grows larger, the separation becomes greater, and there is less likelihood that the system will transfer between the states associated with the two curves. When the modulation amplitude is zero, then the curves do cross (there is then no connection between the successive manifolds), and the system passes diabatically through the two crossing points. In such cases diabatic passage occurs twice, to produce complete population transfer.

When the peak Rabi frequency is larger still, $\varpi_{max} > 2\omega_M$, there may occur overlaps between several of the triads. Figure 5C shows an example of such a case. For such large ratios of ϖ_{max}/ω_M there will occur several pairs of three-state avoided crossings, and several opportunities for failed adiabatic evolution.

It should be noted that, though the evolution may not be adiabatic, it may still happen that the final result of the pulse sequence is successful population transfer. This can happen when evolution diabatically passes through successive curve crossings. This possibility is responsible for some of the special cases of high efficiency.

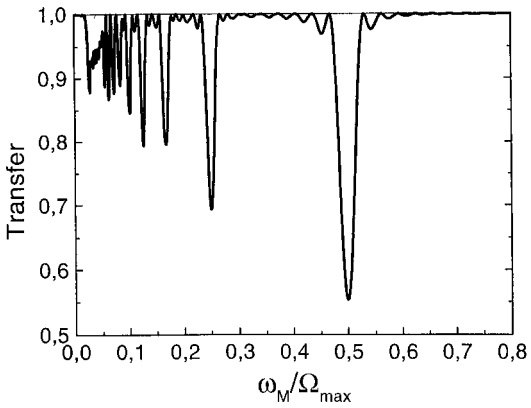

Fig. 6. Population transfer *vs.* ω_M/Ω_{max} for shark-fin pulses. See that large ω_M is good, and for intermediate values there are periodicities. Parameters: shark pulses, pulse area $\Omega_{max}\tau = 200$, modulation amplitude $a_P = a_S = 1$, phases $\phi_P = \phi_S = -0.5\pi$, no loss $\gamma = 0$.

4.4 Adiabatic versus diabatic evolution

There are several possibilities for achieving complete population transfer. One possibility is that the system remain at all times in the transfer state (*i.e.* the adiabatic state which evolves from the initial state) and that this adiabatic state connects with the target state. This is the usual STIRAP procedure; it requires both the maintenance of adiabatic evolution and the connectivity of initial and final states.

There are other possibilities which do not require that the system statevector $\Psi(t)$ remain at all times associated with the same single adiabatic state. If, for example, the quasienergy curve of the transfer state has an avoided crossing with one (or two) other quasienergy curves, then the system may evolve *diabatically* into one of the other adiabatic states. If this state connects with the target state, then successful transfer occurs. Alternatively, the system may undergo a second diabatic change which brings it back into coincidence with an adiabatic state (perhaps the transfer state) which connects to the target state. Pairs of diabatic crossings, for example, can produce complete population transfer.

The need for paired diabatic transitions is quite evident in Figure 5C. We will present below an analytic estimate of probability transfer in such situations.

4.5 Loss

It may happen that, although the system remains adiabatically in the transfer state, and this state connects to the target state, the transfer state has at some times an appreciable component of the excited, lossy state ψ_2. When this is the case, then the loss during the pulse sequence prevents complete population transfer. This is what happens in Figure 4. Even though the modulation frequency is large, so that there occur no avoided crossings of quasienergy curves and the evolution is adiabatic, the transfer state is lossy.

4.6 Pulse shape effects

Although the STIRAP process does not depend sensitively upon pulse shape, it is possible to propose special shapes for which very distinctive results occur. Prior to the start of the pump pulse, the variation of the Stokes pulse is of little interest; so long as the RWA is applicable, it is only with the start of the pump pulse that it becomes important to associate $\Psi(t)$ with an adiabatic state. Similarly, once the Stokes pulse ceases, the subsequent behavior of the pump pulse is not important. Thus it is possible to consider situations in which, at the initial time $t = 0$, the Stokes pulse has a finite value, thereafter diminishing, while at the final time $t = \tau$ when the Stokes pulse vanishes, the pump pulse has a finite value.

One of the most interesting pulse pairs to illustrate pulse-shape effects are the so-called shark-fin pulses (15), in which the Stokes pulse initially starts at its maximum value, following which it falls sinusoidally for one quarter of a sine period. The pump pulse varies cosinusoidally during this quarter period, at the end of which it reaches its peak value. This combination of pulses is of interest because it maintains a constant value of the rms Rabi frequency.

Figure 6 shows the behavior of population transfer for shark-fin pulses as frequency ω_M varies. The plot is remarkable for regular patterns of high and low values. This behavior contrasts with the very irregular appearance of such a plot for Gaussian pulses.

The explanation for this striking regularity can be found by considering the adiabatic Floquet energies. For shark-fin pulses these quasienergies remain constant for all Floquet states. This means, in general, that adiabatic evolution takes place, and transfer efficiency is high. However, when the choice of modulation frequency or peak Rabi frequency causes two states to coincide (as happens whenever ϖ_{max}, which coincides in this case with $\Omega_{max}/2$, is an integer multiple of the modulation frequency) then there occurs a degeneracy of eigenvalues, and population transfer is hindered. This is the explanation for the dips in the curve, which occur when $\Omega_{max}/(2\omega_M)$ is an integer.

4.7 Adiabatic conditions

When the manifolds of quasienergy triads are well separated, we just have the usual adiabatic evolution, in which the system remains identified with one adiabatic Floquet state. For the manifolds to be well separated, the splitting within a triad must be much less than the separation ω_M between triads. The condition for this separation is

$$\tau|\varpi_k - \varpi_n + j\omega_M| \gg 1, \quad k \neq n \tag{22}$$

for all integer j.

When the peak Rabi frequency Ω_{max} is chosen such that ϖ_{max} becomes close to the modulation frequency ω_M

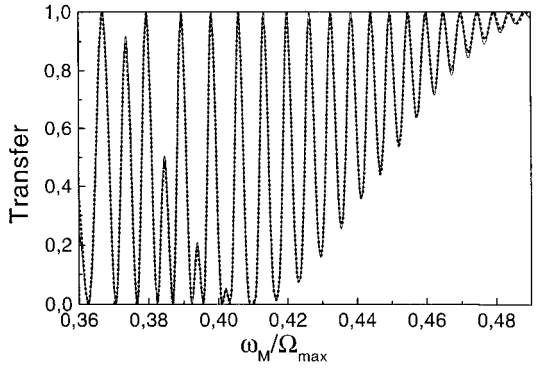

Fig. 7. Population transfer *vs.* ω_M/Ω_{max} for ramp pulses. Solid line is an analytic result of theory, dashed line is numerical result. Parameters: Linear ramp pulses, pulse area $\Omega_{max}\tau = 1500$, modulation amplitude $a_P = 0.1$, $a_S = 0$, phases $\phi_P = -0.5\pi$, $\phi_S = 0$, no loss $\gamma = 0$.

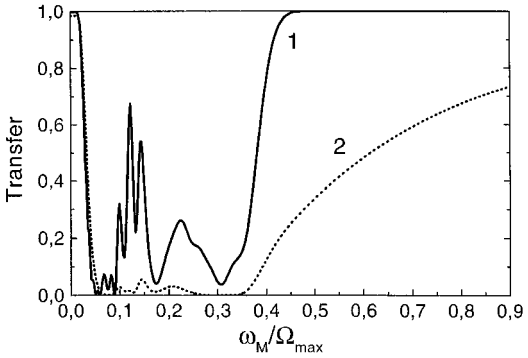

Fig. 8. Population transfer *vs.* ω_M/Ω_{max} for RWA pump pulse and counter-rotating terms in Stokes pulse. The solid-line curve is calculated for no loss, $\gamma = 0$, the dotted curve is calculated for loss $\gamma\tau = 10$. The modulation frequency is $\omega_M = 2\omega_S$. Parameters: Gaussian pulses $\tau_D = \tau$, pulse area $\Omega_{max}\tau = 50$.

then the manifolds begin to affect each other. When ϖ_{max} is much larger than ω_M then the manifolds overlap. There will be crossings or avoided crossings of the curves representing the adiabatic Floquet eigenvalues. As a result, it may not be possible to maintain adiabatic evolution, and good population transfer may not occur (except for special cases).

4.8 Curve crossings

The key to understanding nonadiabatic effects in the present problem is an analysis of the evolution when three eigenvalues become degenerate. This is a three-state generalization of the Landau-Zener two-state model of adiabatic evolution in the presence of a linearly varying energy separation. Analytic results for the three-state Landau-Zener model have been given by Carrol and Hioe [12,13]. Amongst their important results is an expression for the dependence of adiabatic following upon the phase relationships between the three states. We will have two such crossings, and we must consider three-state interference effects as the states evolve between the two crossings.

Appendix A provides analytic expressions (Eqs. (A.16, A.17)) for the efficiency of the population transfer in the case when only pump pulse is modulated ($a_S = 0$) with small amplitude $a_P \equiv a \ll 1$. For the linear ramp pulses (16) these expressions can be significantly simplified:

$$P = \left[(1-2\alpha)^2 - 4\sin(\chi)\alpha(1-\alpha)\right]^2, \quad \alpha \equiv \exp\left(-2\pi p\right), \tag{23}$$

where

$$\chi = \int_{-t_0}^{t_0} dt\, \sqrt{\left(\Omega_0/2 - \omega_M\right)^2 + a^2\Omega_P^{(0)2}\Omega_S^{(0)2}/(16\Omega_0^2)} + 2p(\ln p - 1) - 2\arg\Gamma(ip), \tag{24}$$

$$p = \frac{1}{256}\frac{a^2\Omega_{max}\tau(4\tilde{\omega}^2-1)^2}{\tilde{\omega}\sqrt{8\tilde{\omega}^2-1}}, \quad t_0 = \sqrt{8\tilde{\omega}^2-1}\tau/2, \quad \tilde{\omega} = \omega_M/\Omega_{max}. \tag{25}$$

We have found that expressions (23–25) provide an excellent description of the population transfer when pairs of crossings occur. As an example, Figure 7 shows the population transfer *vs.* ω_M/Ω_{max} for the pulses of equation (16). The solid line is obtained using the formulas (23–25), the dashed line is the numerical result. The parameters of the calculations are $a = 0.1$, $\Omega_{max}\tau = 1500$. One can see extremely good coincidence of the analytical and numerical results.

4.9 Beyond the RWA

One example of pulse modulation occurs when one has an optical transition for the pump and a low frequency transition for the Stokes pulse. Then it is easy to have the Stokes Rabi frequency larger than Stokes frequency itself, whereupon the RWA no longer holds. The needed inclusion of both the rotating and counterrotating terms in the Hamiltonian is an example of the modulation we are considering. For this case we take the pump pulse as

$$\Omega_P(t) = \Omega_P^{(0)}(t) \equiv \Omega_{max} f_P(t) \tag{26}$$

and we incorporate explicit modulation of the Stokes pulse by writing

$$\Omega_S(t) = \Omega_S^{(0)}(t)[1 + \exp(-i\omega_M t)] \tag{27}$$

where $\omega_M = 2\omega_S$ is the modulation frequency. Instead of the modulation $\cos(\omega_M t)$ considered previously, we have here $\exp(-i\omega_M t)$. Hence, we have amplitude and phase modulation simultaneously.

Figure 8 shows the behavior produced by such modulation. As can be seen, the results are qualitatively the same as shown in other figures. However, we draw attention to two features. The first one is the existence of a

critical modulation frequency, above which frequency we have complete transfer (as can be seen from curve 1). The second feature is that when the Stokes frequency is close to the critical one the transfer state has a large admixture of the upper decaying state (as can be seen from curve 2), and so the population transfer will be accompanied by some probability loss.

5 Summary and conclusion

We have examined the effect of putting periodic amplitude modulation onto the pump and Stokes pulses which are used in a STIRAP procedure.

We find that the STIRAP goal, of producing complete population transfer, can be met when certain general conditions are fulfilled by the peak mean Rabi frequency Ω_{max} and the modulation frequency ω_M. In general there is a high transfer efficiency when the modulation frequency exceeds the peak Rabi frequency.

The various results can be understood as an illustration of adiabatic Floquet theory, in which the statevector $\Psi(t)$ remains at all times in an eigenstate of the instantaneous Floquet Hamiltonian. This is a generalization, to a nearly periodic Hamiltonian matrix, of the usual STIRAP analysis involving a quasistatic Hamiltonian matrix.

An important criterion for successful population transfer, namely adiabatic evolution, can be traced on a plot of the dressed eigenvalues of a quasistatic Hamiltonian or on the quasienergies of a Floquet Hamiltonian. In the latter case there occurs an infinite sequence of eigenvalue triplets, each differing by some integer multiple of the modulation frequency ω_M. The interplay between the splitting of a triplet, proportional to the peak mean Rabi frequency Ω_{max}, and the separation of triplets, proportional to ω_M, is responsible for the success or failure of adiabatic evolution and population transfer.

We are grateful for numerous discussions of Floquet theory with Stéphane Guérin. BWS thanks the Alexander von Humboldt Stiftung for a Research Award; his work is supported in part under the auspices of the U.S. Department of Energy at Lawrence Livermore National Laboratory under contract W-7405-Eng-48. LY is grateful to the Deutsche Forschungsgemeinschaft for support of his visit to Kaiserslautern. His work and that of VR was supported by the State Foundation of Fundamental Researches of Ukrainian Ministry of Sciences and Technology (grant 2.4/179). We are grateful for partial support by the EU network "Laser Controlled Dynamics of Molecular Processes and Applications", ERB-CH3-XCT-94-0603. BWS and KB also acknowledge support through a NATO collaborative research grant.

Appendix A: Analytical result

Let us consider the simplest case when only the pump pulse is modulated, with $a_S = 0$, $a_P \equiv a$, $\varphi_P = 0$ and all detunings are equal to zero: $\Delta_P = \Delta_S = 0$. In this appendix we assume that a is small, $a \ll 1$, and will develop a perturbation theory for the small modulation amplitude a in the RWA. (If the a_i are not small one must use Floquet theory for the analysis of the population transfer efficiency.) The Hamiltonian $H(t)$ (3) in this case can be written as

$$H(t) = H_0(t) + H_{int}(t),$$

where

$$H_0(t) = \frac{\hbar}{2}\begin{bmatrix} 0 & \Omega_P^{(0)}(t) & 0 \\ \Omega_P^{(0)}(t) & 0 & \Omega_S^{(0)}(t) \\ 0 & \Omega_S^{(0)}(t) & 0 \end{bmatrix}, \tag{A.1}$$

$$H_{int}(t) = \frac{\hbar}{2}\begin{bmatrix} 0 & a\Omega_P^{(0)}(t)\cos\omega_M t & 0 \\ a\Omega_P^{(0)}(t)\cos\omega_M t & 0 & 0 \\ 0 & 0 & 0 \end{bmatrix}. \tag{A.2}$$

The amplitudes $C_n(t)$ of the dressed states in the expansion (7) satisfy the equations

$$i\hbar\frac{d}{dt}C_n = \sum_m C_m\left[\langle n|H_{int}|m\rangle - i\left\langle n\left|\tfrac{\partial}{\partial t}\right|m\right\rangle\right] \times \exp\left\{-i\int^t dt'\left[\varpi_m(t') - \varpi_n(t')\right]\right\} \tag{A.3}$$

where the eigenvalues $\varpi_m(t)$ are separated by the rms Rabi frequency of the pulse, $\Omega_0(t)$,

$$\varpi_0(t) = 0,$$
$$\varpi_\pm(t) = \pm\frac{1}{2}\sqrt{\left[\Omega_P^{(0)}(t)\right]^2 + \left[\Omega_S^{(0)}(t)\right]^2} \equiv \pm\frac{1}{2}\Omega_0(t). \tag{A.4}$$

The terms on the right hand side of (A.3) proportional to $\left\langle n\left|\frac{\partial}{\partial t}\right|m\right\rangle$ describe the nonadiabatic coupling between dressed states, and the terms proportional to $\langle n|H_{int}|m\rangle$ lead to the coupling between these states due to the periodic perturbation. Hereafter we neglect the nonadiabatic coupling. This means that in the absence of the modulation, $a = 0$, the population of the state ψ_3 after the interaction with the laser pulses is equal to unity. Equation (A.3) then reads

$$i\hbar\frac{d}{dt}C_n = \sum_m C_m\langle n|H_{int}|m\rangle \times \exp\left\{-i\int^t dt'\left[\varpi_m(t') - \varpi_n(t')\right]\right\}. \tag{A.5}$$

Let us consider only "one-photon transitions" between dressed states. This means that during the action of the lasers the conditions

$$\frac{1}{2}\Omega_{min} < \omega_M < \frac{1}{2}\Omega_{max} \tag{A.6}$$

and

$$\frac{1}{4}\Omega_{max} < \omega_M \tag{A.7}$$

are satisfied, where Ω_{max} and Ω_{min} are the maximum and minimum values of the rms Rabi frequency $\Omega_0(t)$. The equation $\Omega_0(t)/2 = \omega_M$ then has two real roots. In this case one can seek the solution of (A.5) as

$$C_0(t) = \tilde{C}_0(t),$$
$$C_\pm(t) = \mp\tilde{C}_\pm(t)\exp\left[\mp i\omega_M t \pm i\frac{1}{2}\int^t dt'\Omega_0(t')\right]. \tag{A.8}$$

Substituting (A.8) into (A.5) and neglecting the terms oscillating with frequency $2\omega_M$ (the RWA) one obtains the equations

$$i\frac{d}{dt}\begin{bmatrix}\tilde{C}_{+1}\\ \tilde{C}_0\\ \tilde{C}_{-1}\end{bmatrix} = \frac{1}{2}\begin{bmatrix}(\Omega_0 - 2\omega_M) & -\bar{\Omega} & 0\\ -\bar{\Omega} & 0 & -\bar{\Omega}\\ 0 & -\bar{\Omega} & -(\Omega_0 - 2\omega_M)\end{bmatrix}\begin{bmatrix}\tilde{C}_{+1}\\ \tilde{C}_0\\ \tilde{C}_{-1}\end{bmatrix}, \tag{A.9}$$

where

$$\bar{\Omega} \equiv \frac{a}{2\sqrt{2}}\frac{\Omega_P^{(0)}\Omega_S^{(0)}}{\Omega_0} \tag{A.10}$$

is the effective coupling between dressed states due to the modulation.

The maximum coupling between dressed states takes place at the instants t when an effective detuning $(\Omega_0/2 - \omega_M)$ is equal to zero. Due to conditions (A.6, A.7) there are two roots, $t = t_{1,2}$, of the equation $(\Omega_0 - 2\omega_M) = 0$. These represent the two times at which curves cross. Far from either crossing (for t far from $t_{1,2}$), one can consider the evolution of the system as adiabatic; the main transitions take place at $t = t_{1,2}$. In the vicinity of $t = t_1$ the equations (A.9) can be written as

$$i\frac{d}{dt}\begin{bmatrix}\tilde{C}_{+1}\\ \tilde{C}_0\\ \tilde{C}_{-1}\end{bmatrix} = \frac{1}{2}\begin{bmatrix}2r_1(t-t_1) & -\Omega_1 & 0\\ -\Omega_1 & 2r_2(t-t_1) & -\Omega_1\\ 0 & -\Omega_1 & 2r_3(t-t_1)\end{bmatrix}\begin{bmatrix}\tilde{C}_{+1}\\ \tilde{C}_0\\ \tilde{C}_{-1}\end{bmatrix}, \tag{A.11}$$

where

$$r_1 = -r_3 = \left|\frac{d\Omega_0}{dt}\right|_{t=t_1}, \qquad r_2 = 0,$$

and $\bar{\Omega}_1 = \bar{\Omega}(t_1)$. The equations (A.11) have *exactly* the same form as equation (1) in the paper of Carroll and Hioe [12], where analytic formulas for the transitions probabilities are derived. Using their results for the initial conditions $\tilde{C}_{\pm1}(-\infty) = 0$, $\tilde{C}_0(-\infty) = 1$ one can write the amplitudes $\tilde{C}_i(t)$, after passing the avoided crossing of three eigenvalues $\varpi_m(t)$, as

$$\tilde{C}_{\pm1}^{(1)} = 2\sqrt{\sinh(\pi p_1)}\exp\left(-\frac{3}{2}\pi p_1 \mp i\varphi_1 - i\pi/2\right)$$
$$\tilde{C}_0^{(1)} = 2\exp(-2\pi p_1) - 1. \tag{A.12}$$

The amplitude exponents p_i and phases φ_i appearing here are

$$p_i = \left(\bar{\Omega}_i\right)^2 / \left[8\left|\frac{d\Omega_0}{dt}\right|_{t=t_i}\right], \tag{A.13}$$

$$\varphi_i = p_i(\ln p_i - 1) - \arg\Gamma(ip_i) + i\pi/4. \tag{A.14}$$

In the time interval between the curve crossings t_1 and t_2 the solutions merely acquire additional phases; they can be written as

$$\tilde{C}_{\pm1} = \tilde{C}_{\pm1}^{(1)}\exp\left[\mp i\int_{t_1}^{t} dt\sqrt{(\Omega_0/2 - \omega_M)^2 + \bar{\Omega}^2/2}\right]$$
$$\tilde{C}_0 = \tilde{C}_0^{(1)}. \tag{A.15}$$

Finally, after the second avoided crossing at the moment $t = t_2$, the population of the state Φ_0 and, hence, the efficiency P of the population transfer, is

$$P = \Big\{[2\exp(-2\pi p_1) - 1][2\exp(-2\pi p_2) - 1] - 8\sqrt{\sinh(\pi p_1)\sinh(\pi p_2)}\exp\left[-\frac{3}{2}\pi(p_1 + p_2)\right]\sin(\chi)\Big\}^2, \tag{A.16}$$

$$\chi = \frac{1}{2}\int_{t_1}^{t_2} dt\sqrt{(\Omega_0 - 2\omega_M)^2 + 2\bar{\Omega}^2} + p_1(\ln p_1 - 1) + p_2(\ln p_2 - 1) - \arg\Gamma(ip_1) - \arg\Gamma(ip_2). \tag{A.17}$$

References

1. U. Gaubatz, P. Rudecki, S. Schiemann, K. Bergmann, J. Chem. Phys. **92**, 5363 (1990).
2. S. Schiemann, A. Kuhn, S. Steuerwald, K. Bergmann, Phys. Rev. Lett. **71**, 3637 (1993).
3. B.W. Shore, K. Bergmann, in *Molecular Dynamics and Spectroscpy by Stimulated Emission Pumping*, edited by H.L. Dai, R.W. Field (World Scientific, Singapore, 1995).
4. A. Kuhn, S. Schiemann, G.Z. He, G. Coulston, W.S. Warren, K. Bergmann, J. Chem. Phys. **96**, 4215 (1992).
5. B.W. Shore, *The Theory of Coherent Atomic Excitation*, Sect. 13.1 (Wiley, N.Y., 1990).
6. J. H. Shirley, Phys. Rev. B **138**, 979-987 (1965).
7. Ya.B. Zeldovich, Zhurn. Exper. Teoret. Fiziki (JETP, USSR) **51**, 1492 (1966).
8. H. Sambe, Phys. Rev. A, **7**, 2203 (1973).
9. W. R. Salzman, Phys. Rev. A **10**, 461 (1974).
10. S.R. Barone, M.A. Narcowich, F.J. Narcowich, Phys. Rev. **15**, 1109 (1977).
11. H.P. Breuer, M. Holthaus, Phys. Lett. A **140**, 507 (1989).
12. C.E. Carroll, F.T. Hioe, J. Opt. Soc. B **2**, 1355 (1985).
13. C.E. Carroll, F.T. Hioe, J. Phys. A **19**, 2061 (1986).